

16<sup>th</sup> Australasian Fluid Mechanics Conference  
Crown Plaza, Gold Coast, Australia  
2-7 December 2007

## Visualization of Submerged Cavitating Jet: Part One –The Phenomenon, Time-Synchronization, Photo Objectives and Sono-Luminescence

E.A. Hutli<sup>1</sup> (MSc), M. Nedeljkovic<sup>2</sup> (Professor) and Vojislav Ilic<sup>3</sup> (PhD)

<sup>1,2</sup>Department of Hydraulic Machinery and Energy Systems  
Belgrade University, Faculty of Mechanical Engineering, Belgrade, Serbia

<sup>3</sup>School of Engineering, University of Western Sydney, Australia

### Abstract

In order to study the jet structure and the behavior of cloud cavitation within time and space, visualization of highly submerged cavitating water jet has been done using 4-Quik-05 camera. This included obligatory synchronization technique and several types of lenses. The influencing parameters, such as: injection pressure, downstream pressure and cavitation number were experimentally proven to be very significant. The recordings of sono-luminescence phenomenon proved the bubble collapse everywhere along the jet trajectory. In addition, the effect of temperature on sono-luminescence was investigated.

### Introduction

Over the past few years, cavitating fluid jets have received considerable attention, primarily with laboratory experiments. If the unsteady behaviour and the jet structure are clarified in detail, as may be expected, the jet working capacity drastically improved [2,8]. Recently, the cavitating jet is used in many fields such as cleaning paint and rust from metal surfaces, underwater removal of marine fouling; removing of high explosives from munitions, augmenting the action of deep-hole mechanical drilling for petroleum or geothermal energy sources. It is also widely used in cutting, penning and flushing. The cavitation clouds produced by cavitating jet always behave stochastically both in time and space, with a very rapid change within  $\mu\text{s}$  [1-5,7,8, 10]. In this paper visualization of high velocity, submerged cavitating water jet was done using a 4-Quik-05 camera with several types of lenses at certain hydrodynamic conditions. The test rig is shown in Fig.1 while Fig 2 shows the test chamber and the cavitating jet impinging on the specimen.

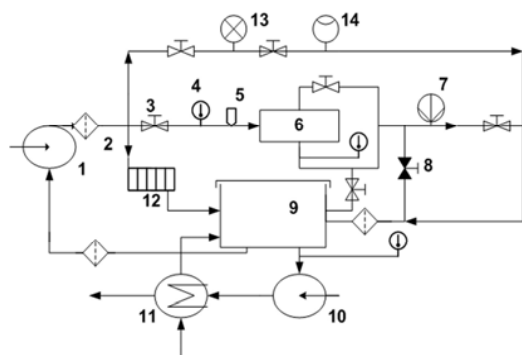


Figure 1. Schematic diagram of Cavitating jet test rig, (1-Plunger pump, 2-Filter,3-Regulation valve,4-Temperature sensor,5-High-pressure transducer, 6-Test-chamber, 7-Low- pressure transducer, 8-Safety valve,9-Reservoir,10-Circulation pump, 11-Heat Exchanger,12-Excess energy dissipator, 13-Pressure gauge, 14 - Flow indicator).

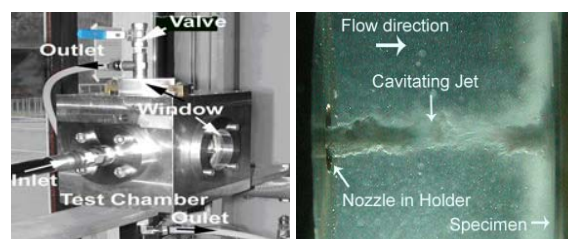


Figure 2. Left - Test chamber, Right - Cavitating jet impinging on the specimen.

### Visualization Of Cavitating Jets Using 4-Quik-05 Camera

The setup with Stanford Optics 4-QUIK-05 equipment through endoscopes with DRELLO 3244 flashlight stroboscope has been used for further visualization analysis. A personal computer equipped with a Matrox video card through a serial port controls the camera. A monitor was connected to the card for the real-time visualization of the results. The 4-Quick-05 camera is a special black-and-white CCD camera with light amplification (ICCD). Its special shutter permits exposure as short as 30 ns. The adjustable gain allows for operations with very low light, but then resolution drops as the gain is increased. Figs. 3 and 4 show the installation of the equipment.

### Synchronization

Because of very rapid changes in the cavitation phenomenon within the order of  $\mu\text{s}$ , and in order to have enough light to illuminate the jet, the shutter and the flash discharge (Drello3244 or Strobex Flash CHADWICK) were synchronized using a photodiode. The photodiode was connected to an oscilloscope, which generates a TTL signal, used to trigger the camera shutter - Fig.4. A second oscilloscope is used to monitor the synchronization of the flash discharge and the trigger signal, Fig.5.

### Visualization of Cavitating Jet Using 4-Quik-05 Camera with Endoscope

Images in Fig.6 were taken with an endoscope. The endoscope lens and the flashlight lamp were mounted together in a same holder tube, as used in medical investigations. This technique was used for two reasons: first, with intention to have the flashlight in the same visualization window (in order to have a homogeneous light distribution in the test chamber and thus to illuminate the whole of the jet uniformly), and secondly to approach the test chamber window wall, i.e. the jet, as close as possible. The obtained images show that this technique is inappropriate for our case. The focusing was inadequate. The

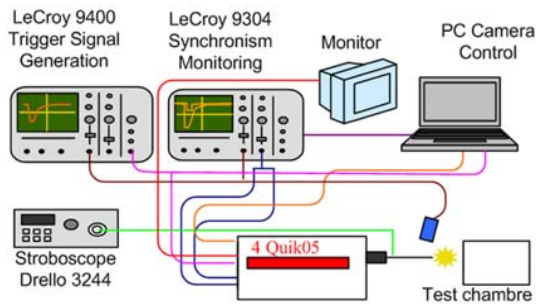


Figure 3. Scheme of the visualization system for the synchronization process. The endoscope is before the test chamber.



Figure 4. The apparatus of the visualization system.

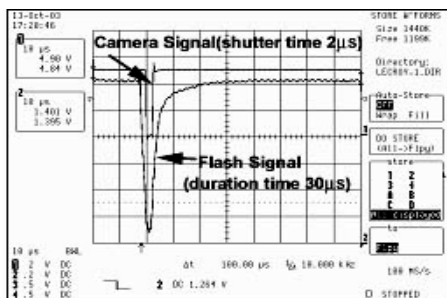


Figure 5. Camera and flash signal synchronization (LeCroy 9304)

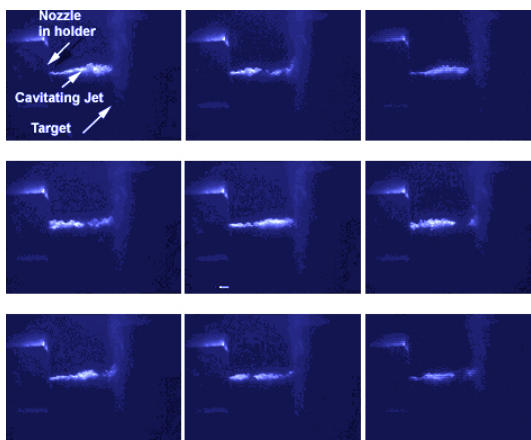


Figure 6. Images obtained with endoscope (Shutter time=1µs and Gain =600V. Conditions,  $P_1=164\text{bar}$ ,  $P_2=0.77\text{bar}$ ,  $V_j=156\text{m/s}$ ,  $\sigma=0.0063$ ,  $T=18^\circ\text{C}$ ).

lens has to be very near to the subject (of the order of a few millimeters) for getting the proper results. The images obtained were used without magnification because of poor resolution. The images in Fig.7 were obtained with 4-Quik 05 camera. The objective used was Cosmicar television Lens 50 mm 1...14, the gain - 600V and the shutter time - 1µs. From group of images in Fig.7 we can notice that, the width of the jet is variable and the jet breaking point position is not at same location in all images because the phenomenon changes within a µs. The strong turbulences of the jet is the main reason for the points mentioned earlier. In addition, along the jet path many bubbles are collapsing, which leads to the change of pressure distribution in the test chamber. Also a many shock waves and micro-jets will be produced as a result of the bubble collapsing- see Figs. 13 and 14. In images of Fig.7, some parts of the jet reflected the flashlight, but in general, the upper part of the jet is brighter than the lower part. This is because the flashlight was directed through the upper window. The rings are not the same in size, but this is normal because every picture represents a certain moment of jet lifetime. As it may be seen in the photos, the cavitating jet is changing with time in the order of µs (as also concluded in [2,5-9]).

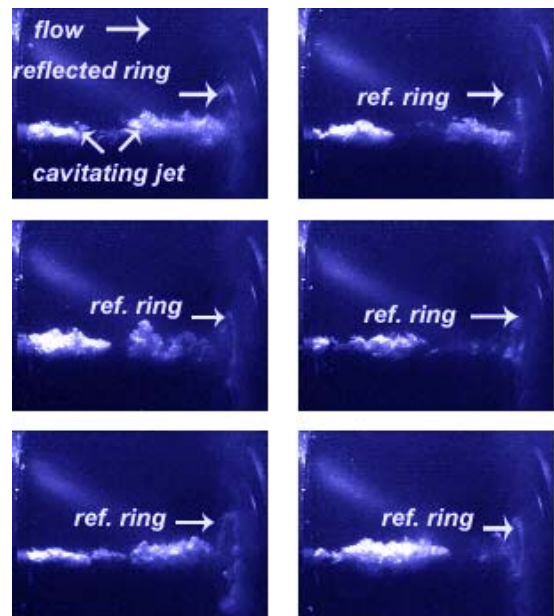


Figure 7. Images were obtained with conditions: ( $P_1=147\text{bar}$ ,  $P_2=0.76\text{bar}$ ,  $V_j=148\text{m/s}$ ,  $\sigma=0.0069$ ,  $T=18^\circ\text{C}$ ).

### Visualization of Cavitating Jet Using 4-QUIK-05 Camera with Magnifier Lenses

In this part, the objective with magnifier lenses was used in order to magnify the jet to get more information. In photos, the jet is divided into three parts which are overlapping as shown in Fig.8. The Navitar Digital Camera Adapter – Navitar's Zoom 6000 system (Navitar 2x adapter (1-6010)(1-6030)(1-60135) magnifier lenses) was used with 4-QUIK-05 camera and the flash light Chadwick-Helmuth Strobex (exposure time 30µs). Visualization has been done two times, once with  $P_2=0.77\text{bar}$ ,  $\sigma=0.0063$  and once with  $P_2=3.04\text{bar}$ ,  $\sigma=0.025$ , where cavitation number was calculated as ( $\sigma = (P_2 - P_v) / (0.5\rho V_j^2)$ ). The results are presented in Figs.9 and 10 respectively. From the images in Figs.10 and 11 (even though the resolution was not the best one), we can easily deduce that all three parts of the jet have dynamic clusters or groups of bubbles, continuously forming and collapsing along

the jet length. The jet surface in all images looks like a rough surface. In some images the flashlight was fully reflected (when the bubbles were spherical), and this is particularly clearer in the images of the jet at  $P_2=0.77$  bar,  $\sigma=0.0063$  than in other images. In addition, we note that the jet width, jet penetration and the number of bubbles increase as  $P_2$  decreases.

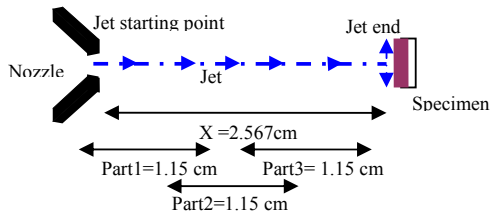


Figure 8. The manner of dividing the cavitating jet during the visualization process using a magnifier objective.

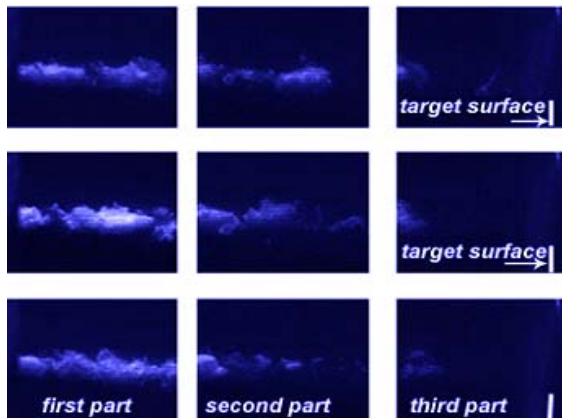


Figure 9. Cavitating jet divided in three zones using magnifier lenses. The gain was 450V and the shutter time was  $1\mu s$ . ( $P_1=164$  bar,  $P_2=0.77$  bar,  $V_j=156m/s$ ,  $\sigma=0.0063$ ,  $T=18^\circ C$ ).

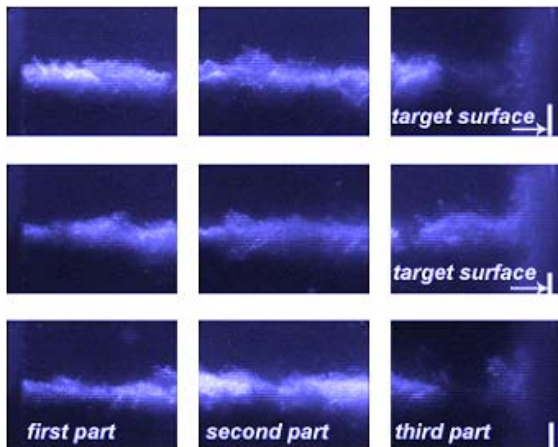


Figure 10. Cavitating jet divided in three zones using the magnifier lenses. The gain was 450V, and the shutter time was  $1\mu s$ . ( $P_1=164$  bar,  $P_2=3.04$  bar,  $V_j=156m/s$ ,  $\sigma=0.025$ ,  $T=18^\circ C$ ).

The amount of bubbles can be deduced from the degree of reflecting light, where the images are brighter at lower values of  $P_2$ . In the case of low  $P_2$ , where the jet can reach the target it can

be seen that at the instant of striking, the jet covers, the entire target wall with a lot of bubbles which are distributed over all target area. Immediately after the striking, the jet is deflected back and the rings appear in the images clearly.

These rings contain a thousands of bubbles, see Fig.12. At high  $P_2$  the jet can not arrive to the end of target distance. It is destroyed before the end of path, and the rings cannot be seen in this case. The repetition of the visualizations was done in order to improve the image quality by playing with the shutter time and the gain value to optimize the image resolution. For instance, hydrodynamic conditions for Figs.11 and 12 were not the same as for Figs.9 and 10.

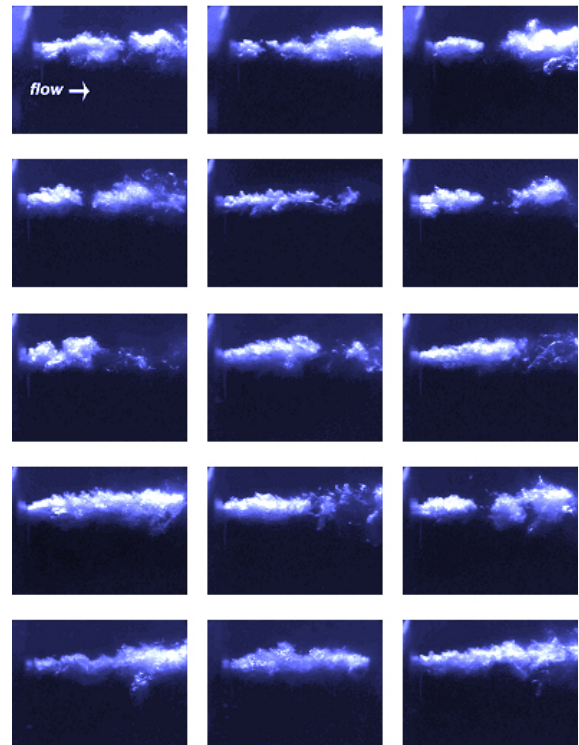


Figure 11. The first part of cavitating jet obtained using magnifier lenses. (Gain = 600V, shutter time =  $1\mu s$ ,  $P_1=164$  bar,  $P_2=3.04$  bar,  $V_j=156m/s$ ,  $\sigma=0.025$ ,  $T=18^\circ C$ ).

### Sono-Luminescence In Cavitating Jet

The attempt to record the sono-luminescence (SL) phenomenon associated to the collapse of bubbles in cavitating jet was also done. The attempts were taken at different values of cavitation number  $\sigma=0.0125$ ,  $\sigma=0.0142$  and  $\sigma=0.0207$ , at constant exit jet-velocity  $V_j$  and working fluid temperature  $T$ . Fig.14 shows representative frames with SL spots registered by the camera. In all shots of SL, the image contrast has been dramatically increased for the reasons of clarity. The aim is to show that the cavity bubbles along the jet path collapse anywhere in and around the jet from its starting point until its end. With this technique, it is possible to identify where the preferred collapse points are located, and how the location and density of the SL bubbles changed with input parameters such as cavitation number or jet velocity. An intensified CCD camera recorded the light emission simultaneously. The intensified camera used (4-QUIK-05) has a standard video output, which can be set to interlaced or non-interlaced operation. The MCP intensifier has a maximum gain of more than 10,000, which should be sufficient to ensure that a recorded photon 'spot' will have a pixel brightness ten

units above the noise level in the CCD. The noise level in the CCD typically did not extend above 29 on a scale of 255 brightness levels (the noise level is determined from the image histogram taken while the intensifier is operated at zero gain), so all levels below 29 were rejected. The camera output was recorded by frame grabber software (Matrox Intellicam). Due to the small fraction of emitted photons, which were intercepted by the camera positioned at the working distance from a jet, relatively few SL flashes were recorded in a single superimposed frame. Due to the values of cavitation numbers, there is no clear difference in density of SL spots between the first and the second image in Fig.13, but the difference exists for the third one. Not all the images obtained using the camera were composed of discrete localised spots of light. Occasionally (once in every few seconds) a comparatively large luminous region would appear in a frame, like in central part of Fig.13. How these events are to be interpreted is unclear. Perhaps the luminous region was far removed from the focal plane of the camera, or a large cavity or cloud of cavities passed over the SL spot. Another possibility would be that the observed extended luminous regions actually were composed of a large number of individual SL bubbles. The collapse of a cloud of cavitation bubbles, for example, might give rise to the effects recorded.

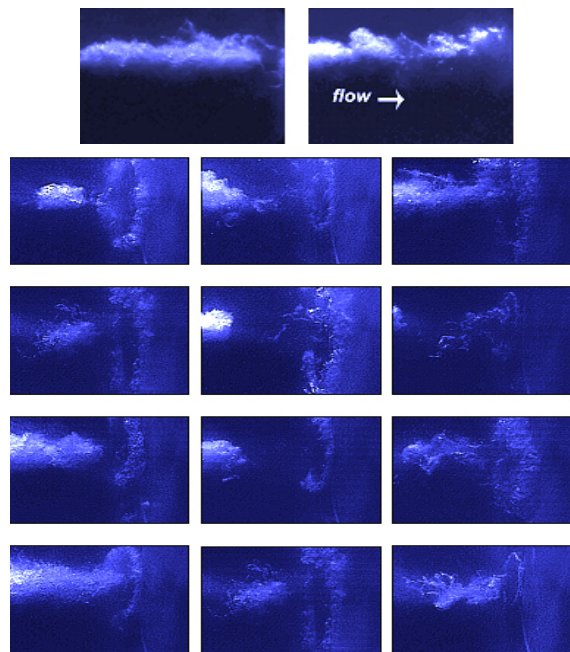


Figure 12. Images of the 2<sup>nd</sup> and 3<sup>rd</sup> part of cavitating jet obtained using magnifier lenses (first two images are for the 2<sup>nd</sup> part). (gain = 600V, and the shutter time =1μs) ( $P_1=164$  bar,  $P_2=3.04$  bar,  $V_j=156$  m/s,  $\sigma=0.025$ ,  $T=18^\circ\text{C}$ ).

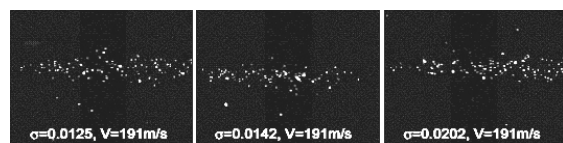


Figure 13. The luminescence phenomenon in a cavitating jet, the flow from left to right, ( $P_1= 213$  bar,  $V_j= 191$  m/s,  $T=22^\circ\text{C}$ ).

In Fig.14 the results were obtained at different working fluid temperatures. It was just an attempt to investigate the influence of

the temperature on the luminescence density and to see does this phenomenon (existence of spherical bubbles) exist or not when the jet is striking on the specimen surface. Ten pictures were superimposed over each one in Fig.14. The density of photons is decreased as temperature increases even this difference was not too much. In addition, there are some spots or photons along the specimen diameter as a ring, i.e. the distribution of the bubbles has the same manner of the defected jet.

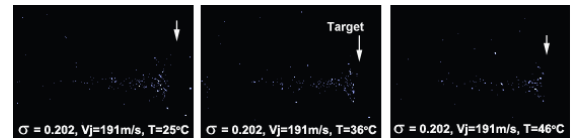


Figure 14. The luminescence phenomenon in a cavitating jet ( $T=25^\circ\text{C}$ ,  $36^\circ\text{C}$  and  $46^\circ\text{C}$ ).

### Conclusion

Cavitating jet is phenomenon changeable with time of  $\mu\text{s}$  order. The jet appears as white clouds with regular frequency. The jet behaviour (penetration length, width, etc) depends on the hydrodynamic conditions, such as cavitation number or  $P_2$  and  $P_1$ . When the cavitating jet strikes the wall, the clouds are formed along the surface area and produce a wall jet. That means that cavitation rings are produced as result of such an action. In general, diameter of the rings depends on hydrodynamic conditions and nozzle geometry. The collapsing of bubbles could not be caught because of inadequate temporal resolution of illuminating and recording system, and the huge number of the bubbles in the cloud cavity (chain production). Catching of the luminescence phenomenon indicates that collapsing of the bubbles takes place everywhere in the jet path. In addition, this proved also the existence of spherical bubbles even for this highly turbulent flow. The kind of visualization system equipment and its resolution is very important to get a good quality of information in the pictures of phenomenon.

### Nomenclature

$\sigma$	cavitation number
	$\sigma = \frac{P_{ref} - P_v}{\frac{1}{2} \rho u_{ref}^2}$
$P_{ref}$	Reference (downstream) pressure (bar)
$P_v(T)$	Saturation (vapor) pressure (bar),
$\rho_L(T)$	Density of the liquid ( $\text{kg/m}^3$ ),
$T$	Fluid temperature [ $^\circ\text{C}$ ]
$u_{ref}$	Reference velocity - exit jet velocity (m/s) $= Q / A = V_j$
$Q$	$= K * \sqrt{(P_1 - P_2)}$ - flow rate ( $\text{m}^3/\text{s}$ )
$A$	Nozzle outlet cross-section area ( $\text{m}^2$ )
$P_1$	Upstream pressure (bar) (absolute)
$P_2$	Downstream pressure (bar) (absolute)
$X$	Stand-off distance (mm)
$L$	Nozzle length
$d_{in}, d_{out}$	Inlet and outlet nozzle diameter (mm)
$K$	$= 4.78\text{E-}09$ for divergent ; $= 6.17\text{E-}09$ for convergent nozzle ( $\text{m}^3/\text{s}/\text{Pa}^{1/2}$ )

### References

[1] Conn AF, Johnson VE, William Jr, Lindenmuth T, Fredrick GS. Some Industrial Applications of Cavitating Fluid Jets

Flow, Proceedings of the First U S A Water Jet Conference Golden, Colorado, 1981

- [2] Keiichi S, Yasuhiro S. Unstable Cavitation Behaviour in a Circular-Cylindrical Orifice Flow. Trans JSME, International Journal, Ser.B, Vol.45, No.3, pp.638-645, 2002
- [3] Koivula T., on Cavitation in Fluid Power, Proceeding of the first FPNI-PhD Symposium, Hamburg 2000, 371-382
- [4] L. Fortunato and A. Torrielli, Theory of light emission in sonoluminescence based upon transitions in confined atoms, The European Physical Journal D - Atomic, Molecular, Optical and Plasma Physics Volume 33, Number 3 pp.315-463, 2005.
- [5] Oba R. The Sever Cavitation Erosion. 2<sup>nd</sup> International Symposium on Cavitation. Tokyo, Japan, 1994.
- [6] Soyama H. High-Speed Observation of a Cavitating Jet in Air, Trans ASME, Journal of Fluids Engineering, November 2005, Vol. 127, pp 1095-1101, 2005.
- [7] Soyama H, Adachi Y, Yamauchi Y, Oba R. Cavitation-Noise-Characteristics Around High Speed Submerged-Water-Jets. Second International Symposium on Cavitation, Tokyo, Japan, 1994.
- [8] Soyama H, Ikohagi T, Oba R. Observation of the Cavitating Jet in a Narrow Watercourse. Cavitation and Multiphase Flow, ASME, FED -Vol. 194, 79-82, 1994.
- [9] Soyama H, Yamauchi Y, Adachi Y, Adachi Y, Oba R. High-Speed Cavitation-Cloud Observations Around High-Speed Submerged Water Jets. The second international Symposium on Cavitation, Tokyo, Japan. 225-230, 1994.
- [10] Toyoda K, Muramatsu Y, Hiramoto R. Visualization of the Vortical Structure of a Circular Jet Excited by Axial and Azimuthal Perturbation, Journal of Visualization, Vol.2 No.1, July, 1999.
- [11] Yamauchi Y, Kawano S, Soyama H, Sato K, Matsudaira Y, Ikohagi T, Oba R. Formation of process of vortex ring cavitation in high-speed submerged water jet. Trans JSME, ser. B, 62-593; 72-78, 1996.